

UNCLASSIFIED

AD NUMBER
ADB075698
NEW LIMITATION CHANGE
TO Approved for public release, distribution unlimited
FROM Distribution authorized to U.S. Gov't. agencies only; Test and Evaluation; 31 DEC 1981. Other requests shall be referred to Commanding Officer, Naval Research Laboratory, Washington, DC 20375.
AUTHORITY
NRL [IPO-11A4] ltr dtd 8 Aug 1997

THIS PAGE IS UNCLASSIFIED

L

2

NRL Report 8568
(Revised 2/22/83)

AD B 0 7 5 6 9 8

A Stochastic Simulation of Low Grazing Angle, Forward Scatter, Over-Water Multipath Effects

D. Y. NORTHAM

*Advanced Techniques Branch
Tactical Electronic Warfare Division*

December 31, 1981

*Superseded
AD-3062837*



NAVAL RESEARCH LABORATORY
Washington, D.C.

DTIC
AUG 11 1983
A

DTIC FILE COPY

Distribution limited to U.S. Government Agencies only, test and evaluation, December 1981. Other requests for this document must be referred to the Commanding Officer, Naval Research Laboratory, Washington, D.C. 20375.

83 08 10 023

REPORT DOCUMENTATION PAGE		READ INSTRUCTIONS BEFORE COMPLETING FORM
1. REPORT NUMBER NRL Report 8568	2. GOVT ACCESSION NO. AD-B075698L	3. RECIPIENT'S CATALOG NUMBER
4. TITLE (and Subtitle) A STOCHASTIC SIMULATION OF LOW GRAZING ANGLE, FORWARD SCATTER, OVER-WATER MULTIPATH EFFECTS	5. TYPE OF REPORT & PERIOD COVERED A final report on one phase of a continuing NRL problem.	
	6. PERFORMING ORG. REPORT NUMBER	
7. AUTHOR(s) D. Y. Northam	8. CONTRACT OR GRANT NUMBER(s)	
9. PERFORMING ORGANIZATION NAME AND ADDRESS Naval Research Laboratory Washington, DC 20375	10. PROGRAM ELEMENT, PROJECT, TASK AREA & WORK UNIT NUMBERS 57-0481-E-1 57-0535-0-1	
11. CONTROLLING OFFICE NAME AND ADDRESS	12. REPORT DATE December 31, 1981	
	13. NUMBER OF PAGES 20	
14. MONITORING AGENCY NAME & ADDRESS (If different from Controlling Office)	15. SECURITY CLASS. (of this report) UNCLASSIFIED	
	15a. DECLASSIFICATION/DOWNGRADING SCHEDULE	
16. DISTRIBUTION STATEMENT (of this Report) Distribution limited to U.S. Government agencies only; test and evaluation; Dec. 1981. Other requests for this document must be referred to the Commanding Officer, Naval Research Laboratory, Washington, DC 20375.		
17. DISTRIBUTION STATEMENT (of the abstract entered in Block 20, if different from Report)		
18. SUPPLEMENTARY NOTES		
19. KEY WORDS (Continue on reverse side if necessary and identify by block number) Multipath Simulation Stochastic models		
20. ABSTRACT (Continue on reverse side if necessary and identify by block number) This report describes a stochastic model and a simulation of low grazing angle, forward scatter, over-water multipath applicable to microwave frequencies. The model is based primarily on the work of Charles Beard, using a coherent and an incoherent vector summation to describe the reflected signal. A second order stochastic model and an associated stochastic simulation are described. Controlling parameters are sea state, radar frequency, transmitter/receiver geometry, and radar antenna patterns. A model is suggested for the incoherent spectrum when one or both radars are moving.		

A STOCHASTIC SIMULATION OF LOW GRAZING ANGLE, FORWARD SCATTER, OVER-WATER MULTIPATH EFFECTS

INTRODUCTION

One of the major concerns of the Tactical Electronic Warfare Division (TEWD) of the Naval Research Laboratory is evaluating the performance of electronic countermeasures (ECM) in defending ships from anti-ship cruise missile (ASCM) attacks. In the Advanced Techniques Branch (Code 5750), digital, pulse-by-pulse simulations of missile-ship engagements are used to study in detail the response of missiles to ECM during such engagements. Because these engagements take place at sea, over-water multipath is often an important factor to consider in such studies. For this reason, Code 5750 has developed and implemented a pulse-by-pulse, digital simulation of low grazing angle, over-water, forward scatter multipath applicable to microwave radar frequencies.

MODEL AND SIMULATION CONSTRAINTS

The over-water multipath phenomenon is of course an extremely complex one to describe in detail. Therefore, it was important to isolate the dominant effects of the phenomenon on the particular ECM studies that Code 5750 anticipated conducting. Further, it was important to develop mathematical models that are amenable to validation (by validation we mean that the model accurately describes the effects to second-order statistics). Finally, the model had to lead to a digital simulation that would be used as a submodule in larger, more comprehensive simulations whose purpose would be ECM evaluation. These general requirements lead to more specific requirements or constraints. Because the simulation was to be a part of several larger pulse-by-pulse simulations, it had to be

- (1) able to generate multipath effects as a time series (pulse-by-pulse),
- (2) fast running, and
- (3) modular, for general applicability and clarity.

Because the applications had to deal with understanding detailed aspects of radar systems performance, the simulation had to

- (4) generate the complex (amplitude and phase) multipath effects, and
- (5) generate receive signals (affected by multipath) accurate to at least second order statistics (i.e., density function, location and spread parameters, and power spectral density).

Because the mathematical model had to be validated, its parameters needed to be

- (6) as few as possible, and
- (7) experimentally measurable.

These constraints have led to the development of a second-order stochastic, phenomenological model, that is, a model that is based on physically measurable parameters and that describes the extremely complex physical processes (the generation of incoherent scattering by a rough sea surface) stochastically.

MULTIPATH MODEL

The stochastic model which we have developed is based primarily on the work of Beard, Katz, and Spetner [1-3]. John Baras developed the original version of the stochastic model described in this report and has also developed several, more sophisticated (detailed) multipath effects models [4] than the one presented in this report. Simulations of the more sophisticated models have not been developed because for each of our application studies to date, we have judged the Beard model to be adequate in its description of multipath effects.

Model Summary

The simulation model is based on the concept of vectors representing the electric field strength at the receive antenna. This field strength is modeled as the sum of two components, a direct path vector and a reflected vector.

Figure 1 illustrates and defines the individual vector components of the model. The direct signal \bar{D} (that received in the absence of multipath effects) is taken as the reference vector. The reflected signal, \bar{R} , is the sum of two other vectors, a coherent (relative to \bar{D}) vector, \bar{C} , and an incoherent vector, \bar{I}^* . The coherent component is the specularly reflected vector which would be received if the sea was perfectly smooth, modified by a scattering coefficient. The incoherent component accounts for the time varying effects of the sea on the receive signal (in particular, the spectrum). The non-time-varying properties of the reflected components are primarily functions of

- (1) the electrical properties of the sea,
- (2) the geometry, and
- (3) the radar wavelength, polarization, and antenna patterns.

The total (vector sum) receive signal is represented by the vector \bar{T} .

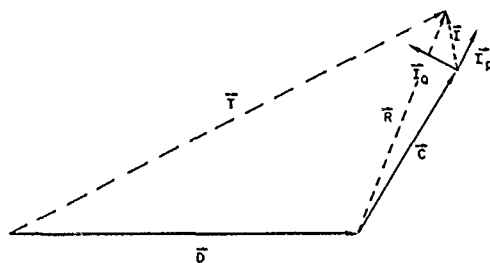


Fig. 1 — Receive signal vector summation

Consider transmit and receive radar antennas fixed relative to the earth, a distance R apart, and at heights above the mean sea level of h_T and h_R , respectively (Fig. 2). If the geometry does not change

*The coherent and incoherent vectors are also referred to as the specular and diffuse vectors, respectively.

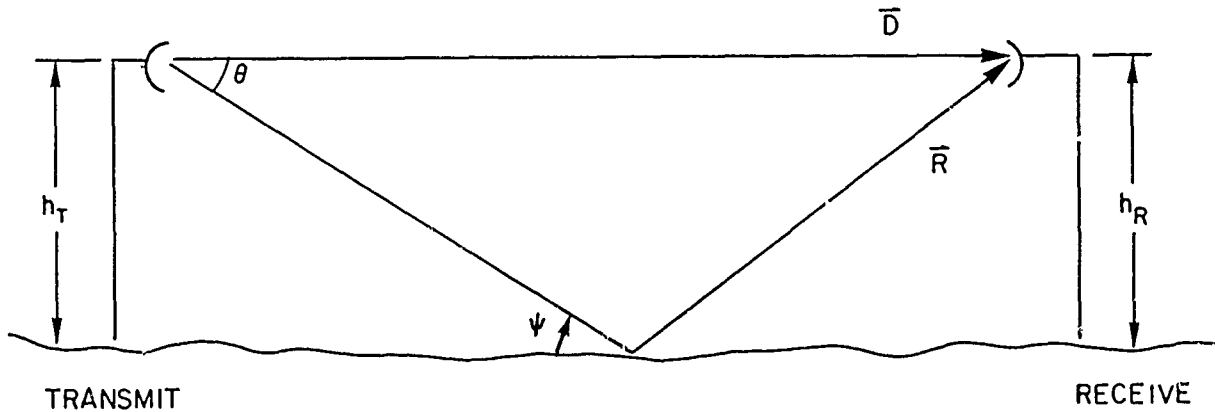


Fig. 2 - Multipath geometry

with time (an assumption that we make to develop the fundamental model) then the only significant variation in the receive signal is due to sea surface motion. This motion directly controls the receive signal variation, and we use a characterization of its second-order properties to determine the receive signal's second-order properties. For our purposes, the sea surface motion can be adequately characterized by a simple representation of the wave height spectrum and a surface roughness parameter g . These two observables are the most fundamental parameters of the model. The roughness parameter used is defined by

$$g = \frac{h \sin \psi}{\lambda} \quad (1)$$

where

- h = RMS wave height (standard deviation)
- ψ = grazing angle
- λ = radar wavelength.

The following sections describe in detail the various components of the simulation model.

Coherent Component

The coherent vector is described by

$$\bar{C} = |\bar{D}| \Gamma \rho_c e^{j \frac{2\pi \Delta R}{\lambda}}, \quad (2)$$

where

- \bar{D} = direct signal
- Γ = smooth sea reflection coefficient (complex)
- ρ_c = coherent scattering coefficient
- ΔR = direct and reflected, path length difference
- λ = radar wavelength.

Antenna pattern effects, not shown in Eq. (2), are discussed in the section devoted to this, and a summary of the calculation of Γ is also given in a later section. Figure 3 is a plot of three models that have been developed to describe ρ_c . Ament's model [5] is

$$\rho_c = e^{-2(2\pi g)^2}, \quad 0 \leq g \leq 0.3. \quad (3)$$

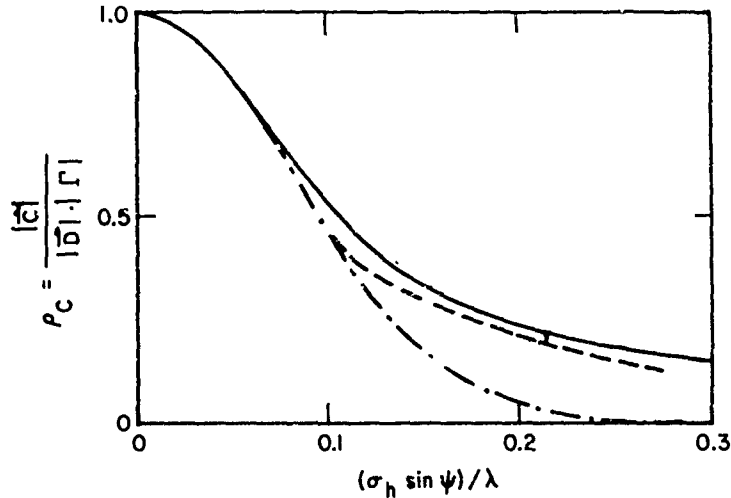


Fig. 3 — Three models for the coherent scattering coefficient (from [6]). Solid line is theory (Brown and Miller), dashed line is approximation to experimental curve (Beard), and dotted line is theory (Ament).

Brown and Miller [6] have derived an expression, using geometrical optics which is a better fit to Beard's data:

$$\rho_c = e^{-2(2\pi g)^2} I_0(2(2\pi g)^2), \quad 0 \leq g \leq 0.3, \quad (4)$$

where $I_0(x)$ is the modified Bessel function $J_0(ix)$. The third model is

$$\rho_c = \begin{cases} \exp[-2(2\pi g)^2], & 0 \leq g \leq 0.1 \\ \frac{0.812537}{1 + 2(2\pi g)^2}, & 0.1 \leq g \leq 0.3 \end{cases}, \quad (5)$$

which is our approximation to the empirical fit made by Beard to experimental data [3]. Models (4) and (5) are implemented in the simulation, and the user has the option of specifying which model to use (when he initializes the simulation).

Incoherent Component

The incoherent vector is assumed to be the resultant sum of vectors from many, independent, random scatterers. Therefore it is represented as the sum of two zero mean Gaussian processes, \bar{I}_P and \bar{I}_Q which are orthogonal (Fig. 1). As in Ref. 1, we assume that \bar{I}_P and \bar{I}_Q are independent although it is known [7] that correlation of \bar{I}_P and \bar{I}_Q can occur due to wave front sphericity. The validity of this assumption is further strengthened by Ref. 8 where it was found that for data collected at the Gulf of Mexico, \bar{I}_P and \bar{I}_Q were independent. For convenience, the phase of \bar{I}_P is assumed to be that of \bar{C} . It is further assumed that the power spectral density of \bar{I}_P and \bar{I}_Q are identical since we know of no physical reason to assume otherwise. Therefore we have

$$\bar{I} = |\bar{D}| \Gamma (\bar{I}_P + \bar{I}_Q). \quad (6)$$

The standard deviation of the processes are identical and are determined by the incoherent scattering coefficient, ρ_I . Figure 4 shows experimental data collected and a curve fit to that data by Beard [3] describing ρ_I as a function of the roughness parameter.

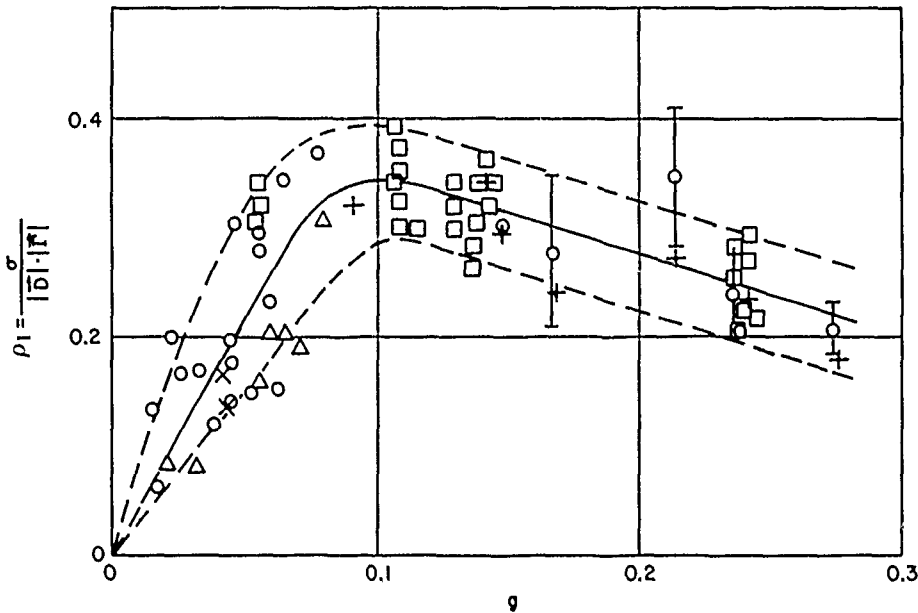


Fig. 4 — Incoherent scattering coefficient or normalized standard deviation (from [3])

In the simulation, the expression

$$\bar{T} = |\bar{D}| |\Gamma| \sqrt{2} \rho_I (I_1 + jI_2) \tag{7}$$

is used to generate \bar{T} . I_1 and I_2 are independent $N(0, 1)$ processes (normalized Gaussian). The $\sqrt{2}$ term arises because the sum of two $N(0, \rho_I)$ processes is a $\sqrt{2}\rho_I N(0, 1)$ process. The receive signal spectrum will be discussed later in detail.

Extrapolation of the Coherent and Incoherent Coefficients

The above models of ρ_c and ρ_I are validated for $g < 0.3$ [3] and at present, the author is unaware of any validated models for $g > 0.3$. This raises two questions: first, what are good models of ρ_c and ρ_I for $g > 0.3$ and second, given the present models, how should one simulate a transition from $g < 0.3$ to $g > 0.3$. When a validated model becomes available it can be directly implemented in the simulation. For our applications, the second problem occurs only as a result of the grazing angle increasing during a simulation (λ and h_{RMS} are fixed during the simulation). This increase in g is usually also accompanied by antenna gain reductions in the reflected signal direction which further reduce the multipath effects. Therefore for our purposes, we assume that whatever ρ_c and ρ_I are when g increases beyond 0.3, they are, for practical purposes, nonincreasing and small. In the simulation we have extrapolated the ρ_c and ρ_I models as described in the following paragraph.

Assuming minimal multipath effects for $g > 0.3$, we suggest three practical approaches to simulating the transition of ρ_c and ρ_I through $g = 0.3$. First, one can simply not calculate multipath terms for $g > 0.3$. Because this introduces discontinuities in the pulse-by-pulse signal synthesis (at $g = 0.3$) and because there are probably some "residual" multipath effects for large values of g , we have taken a second approach. Currently in the simulation we make smooth extrapolations of both ρ_c and ρ_I . ρ_c is extrapolated by extending (4) and (5) to all values of g , and ρ_I is a linear extrapolation (Fig 5) of the

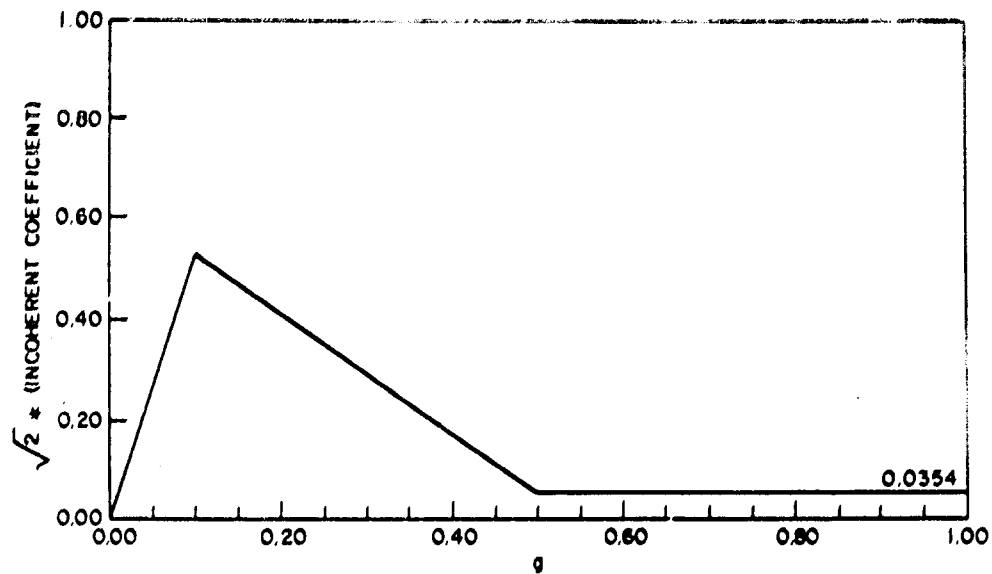


Fig. 5 - Extrapolation of the incoherent coefficient

linear fit in Fig. 4. The third method is to smoothly extrapolate the two coefficients to zero at some $g = g_{max} > 0.3$ and not calculate any multipath terms (which would be zero) for $g > g_{max}$.

Reflection Coefficient for a Smooth Plane Surface

Here we summarize the model of the reflection coefficient following Chapters 2 and 5 of Ref. 9. There are two expressions for the coefficient depending on the radar polarization:

$$\Gamma_{\perp} = \frac{\epsilon_c \sin \psi - \sqrt{\epsilon_c - \cos^2 \psi}}{\epsilon_c \sin \psi + \sqrt{\epsilon_c - \cos^2 \psi}} \quad (8)$$

for vertical polarization and

$$\Gamma_{\parallel} = \frac{\sin \psi - \sqrt{\epsilon_c - \cos^2 \psi}}{\sin \psi + \sqrt{\epsilon_c - \cos^2 \psi}} \quad (9)$$

for horizontal polarization where ψ is the grazing angle and ϵ_c is the complex dielectric constant which we approximate by

$$\epsilon_c = \epsilon - 60\lambda\sigma l \quad (10)$$

where

- ϵ is sea dielectric constant,
- λ is radar wavelength (m), and
- σ is sea conductivity (mho/m).

Based on Table 5.1 of Ref. 9, we have chosen to use seawater values of $\sigma = 4.3$ mho/m and $\epsilon = 80$. Simulations of (8) and (9) have shown that for our applications, variations in Γ_{\parallel} and Γ_{\perp} due to variations in ϵ and σ about these values are not significant. Figures 6 through 9 illustrate the character of the amplitude and phase of Γ_{\perp} and Γ_{\parallel} as a function of grazing angle for fixed λ , σ , and ϵ .

Fig. 6 - $|\Gamma_H|$; $\lambda = 2.5$ cm, $\sigma = 4.3$ mho/m,
 $\epsilon = 80$

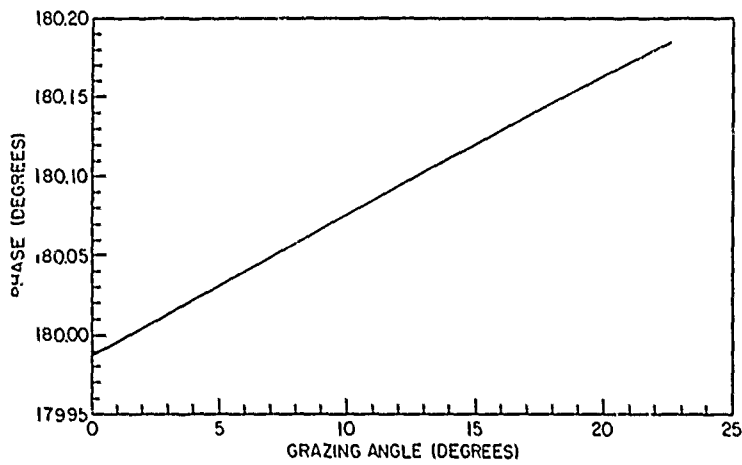
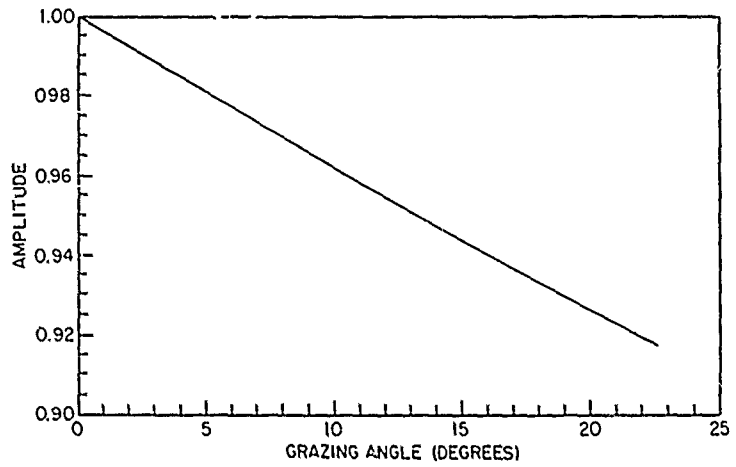
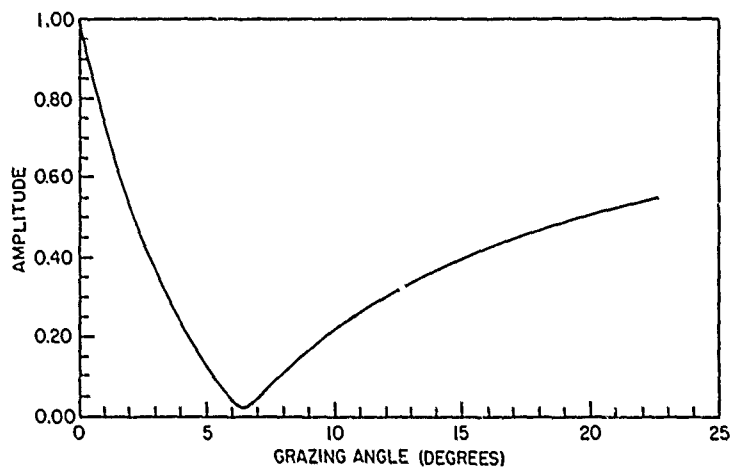


Fig. 7 - Angle of Γ_H ; $\lambda = 2.5$ cm, $\sigma = 4.3$
mho/m, $\epsilon = 80$

Fig. 8 - $|\Gamma_V|$; $\lambda = 2.5$ cm, $\sigma = 4.3$ mho/m,
 $\epsilon = 80$



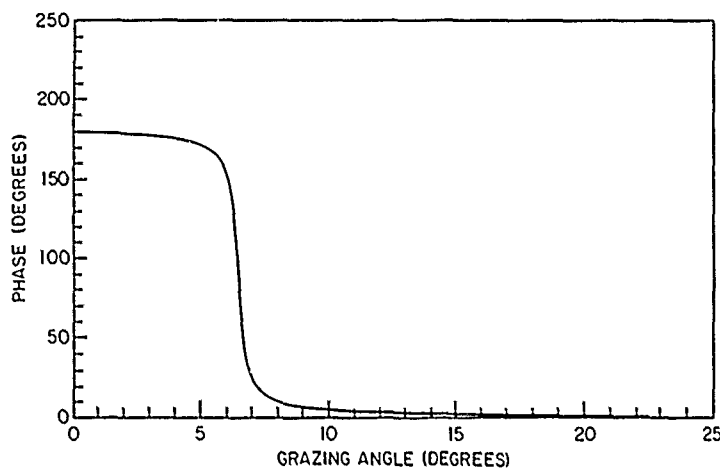


Fig. 9 — Angle of Γ_V ; $\lambda = 2.5$ cm, $\sigma = 4.3$ mho/m, $\epsilon = 80$

The calculation of Γ is, relatively, very time consuming and variations in Γ due to small changes in grazing angle are also small. Therefore we include in the simulation a test to decide when to recalculate Γ rather than performing a pulse-by-pulse calculation. This is particularly efficient for stationary platform studies. The thresholds (indicating significant grazing angle change) used were determined by examining Γ where the rate of change of Γ was most significant. A threshold of 1° change was chosen for Γ_H (somewhat arbitrarily due to the minimal variations in the amplitude and phase of Γ_H). An examination of the Γ_V angle curve indicates that as much as a 180° phase change can occur for about a 1° grazing angle change. Therefore, a value of 0.01° is used in the simulation as an update threshold for calculating Γ_V .

Receive Signal Spectrum

Up to this point we have described only the first-order properties of the receive signal (RS). To complete the second-order model, we need a description of the RS spectrum (or autocorrelation function).

For our applications, we place two requirements upon the character of the RS variations:

- (1) for fixed geometry (Fig. 2), the RS must be statistically stationary, and
- (2) wave height directionality must not be a parameter of the RS variations (our applications require an "average effect" with respect to wave directionality).

These requirements will be assumed throughout the following paragraphs.

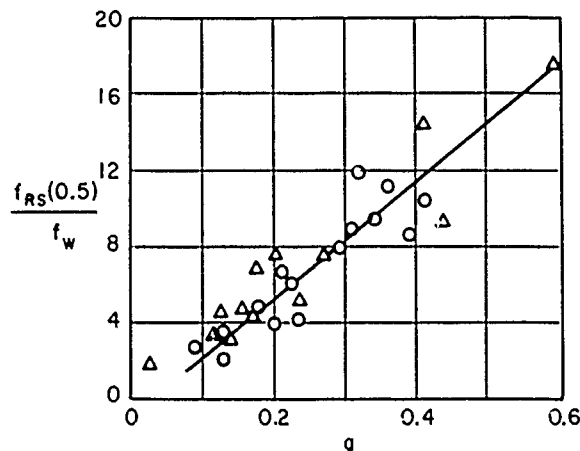
When the geometry is fixed, the fluctuations in the RS are due to the motion of the sea surface. Therefore, the various characteristics of the RS fluctuations should be directly related to the associated characteristics of the sea surface variations. This intuitive idea has been quantitatively verified [2,8,10,11]. In particular, the experimental work described in Ref. 10 indicates that the RS spectrum is, in fact, strongly related to the wave height (WH) spectrum.* In particular, both spectra have been shown to possess at least for relatively low sea states, the same qualitative shape. Each spectrum has what may roughly be described as a "bandpass shape"; that is they can be characterized, in large measure, by specifying a center frequency, a bandwidth, and a process variance.

* A detailed quantitative analysis of these data has not been conducted to date. However it is anticipated that such work will be undertaken in the near future.

For our simulation we have chosen to generate the spectrum of the RS process by modeling the spectra of the incoherent components as bandpass spectra. This was done for two reasons. First, bandpass processes can be easily and efficiently generated digitally and second, although it is known that the WH and RS spectra are related, a precise quantitative description of the RS spectrum is not yet known. However, the following approximate results have been found experimentally:

- (1) the upper 3 dB frequency of the RS spectrum is linearly related (Fig. 10) to the ~~upper 3 dB~~ ^{center} frequency of the WH spectrum [2], and
- (2) the RS spectrum center frequency is approximately equal to the WH spectrum center frequency [10].

Fig. 10 — Relationship between RS spectrum upper 3 dB point and f_W and g (from [2])



Further, by using a series expansion of the magnitude of the total receive signal \bar{T} (Fig. 1), Beard and Katz [2] have shown that

- (3) when \bar{D} and \bar{C} are in phase, to first order, the spectrum of $|\bar{T}_P|$ is equal to the spectrum of $|\bar{T}|$.

Our approach to generating the spectrum of the RS process, based on the above three results, is.

- (1) Choose a sea state.
- (2) Based on the chosen sea state, pick a representative WH spectrum.
- (3) Calculate a center frequency, f_W , ~~and the upper 3 dB frequency, $f_{RS}(0.5)$~~ , for the WH spectrum.
- (4) To generate the RS process with appropriate spectrum, generate \bar{T}_P and \bar{T}_Q processes which have bandpass spectra each with center frequency f_W (from result (1) above), upper 3 dB frequency $f_{RS}(0.5)$ (from result (2) above), and variance $\sqrt{2} \cdot \rho_I$ (from the section describing the incoherent component).

Summing \bar{D} and \bar{C} vectors with \bar{T}_P and \bar{T}_Q as described above produces a power process $|\bar{T}|^2$ whose second order statistics match closely the second-order statistics of experimental data collected by Code 5750.

Although various models of WH spectra exist, for our purposes we need only a model that will yield an estimate of f_W for a given sea state or a given wind speed. For this we use the Neumann spectrum [12] which is defined by

$$A^2(f) = \frac{C_1}{f^6} e^{-C_2 \left(\frac{1}{Vf}\right)^2} \tag{11}$$

where

V = wind speed (knots)

f = frequency (Hz)

C_1 = 0.779

$C_2 = \left(\frac{g_e}{2\pi}\right)^2$

$g_e = 32.2 \text{ ft/s}^2$.

The general form of this spectrum is shown in Fig. 11. Equation (11) can be used to obtain the center frequency f_W by setting the derivative of $A^2(f)$ to zero and solving for f_W . This yields

$$f_W = \frac{2.476}{V}. \tag{12}$$

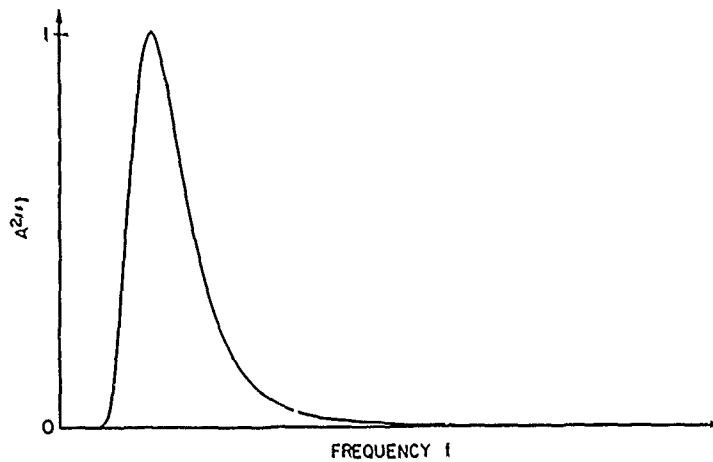


Fig. 11 - General form of the Neumann Spectrum

The variance of the WH process (required for the calculation of g) can be estimated by integrating the assumed (Neumann) WH spectrum. Using the standard symbol E , the variance is [13]

$$\text{Var} = \frac{E}{2},$$

where

$$E = 0.242 \left(\frac{V}{10}\right)^5, \tag{13}$$

and

$$V = \text{wind speed (knots).}$$

From Eq. (13) we obtain the RMS wave height (WH standard deviation) as

$$h_{RMS} = 0.00110 V^{5/2}. \quad (14)$$

Finally, we use the power-point/center-frequency/sea-roughness curve of Fig. 12 to obtain $f_{RS}(0.5)$. The straight line portion of this curve is based on Fig. 10 ($g \geq 0.1$). We have implemented a smooth interpolation (using a $C_1 + C_2g^{C_3}$ fit) from $g = 0.1$ to $g = 0.0$. This allows continuous variations of $f_{RS}(0.5)$ in the simulation.

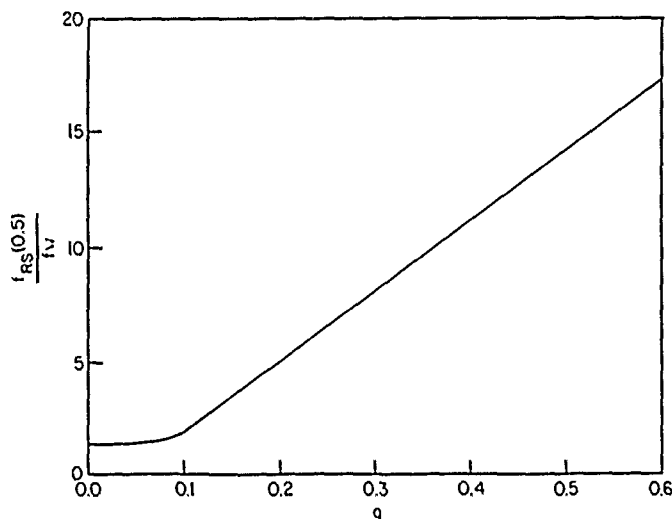


Fig. 12 — Calculation of $f_{RS}(0.5)$ from sea roughness and wave spectrum center frequency

In general, our studies use one of three nominal sea conditions: slight, moderate, or rough. To obtain h_{RMS} , $f_{RS}(0.5)$, and f_H for a given sea state we first chose a wind speed appropriate to the sea state, then calculate the above parameters. The values of wind speed that we typically use along with values of associated parameters are shown in Table 1.

Table 1 — Typical Values of Sea Surface Parameters for Three Sea Conditions

Sea state	Wind speed (knots)	h_{RMS} (feet)	h_{RMS} (meters)	BW_W (Hz)	f_W (Hz)
Slight (SS2)	7	0.14	0.043	0.26	0.354
Moderate (SS3)	11	0.44	0.135	0.16	0.225
Rough (SS4)	21	2.22	0.678	0.09	0.118

Generation of the Incoherent Processes

The fundamental stochastic processes that we generate in the simulation are the incoherent components \bar{I}_p and \bar{I}_Q . As stated before, for the fixed platform model the processes will be wide-sense stationary, zero-mean Gaussian, and independent. Because the processes have bandpass spectra, they will have autocorrelation functions of the form

$$R(\tau) = \exp(-\alpha\tau) \cos \omega\tau. \quad (15)$$

This form and the requirement that a fast digital simulation be developed led us to use first-order, Gauss-Markov random sequences to generate the processes. A detailed analysis of such sequences is given in Ref. 14.

We begin the description of the process generation by describing the generation of an exponentially correlated, Gaussian sequence X_K (see also Ref. 14). Let W_K be a Gaussian, white noise sequence with

$$\left. \begin{aligned} E\{W_K\} &= 0 \\ E\{W_K W_l\} &= \begin{cases} 1, & k = l \\ 0, & k \neq l \end{cases} \end{aligned} \right\} \quad (16)$$

Then the values of the process at time K can be approximated by

$$\left. \begin{aligned} X_K &= AX_{K-1} + BW_K \\ \text{where} \quad E\{X_0\} &= 0 \\ E\{X_0^2\} &= R_X(0) = R_0 \end{aligned} \right\} \quad (17)$$

We need to find values for A and B . By calculating the covariance of X_K , one can show [14] that the covariance will be stationary if

$$\left. \begin{aligned} 0 \leq A < 1, \text{ and} \\ R_0 &= \frac{B^2}{1 - A^2} \end{aligned} \right\} \quad (18)$$

This defines B in terms of R_0 and A . Next, we require that

$$E\{X_0 X_{\Delta t}\} = R_0 \exp(-2\Delta t) \quad (19)$$

where Δt is the simulation step size. We also have

$$\begin{aligned} E\{X_0 X_{\Delta t}\} &= E\{X_0 (AX_0 + BW_{\Delta t})\} \\ &= AE\{X_0^2\} + BE\{X_0 W_{\Delta t}\} \\ &= AR_0 \end{aligned}$$

so that A is determined:

$$R_0 \exp(-\alpha\Delta t) = AR_0,$$

or

$$A = \exp(-\alpha\Delta t). \quad (20)$$

Finally, using R_0 from Eq. (17) the X_K process is stationary since

$$\left. \begin{aligned} E\{X_K\} &= 0, \\ \text{and [14],} \quad E\{X_K X_{K+l}\} &= \frac{B^2}{1 - A^2} |\alpha|^l. \end{aligned} \right\} \quad (21)$$

We now have a method of generating a first-order, Gauss-Markov sequence with autocorrelation $R_0 \exp(-\alpha t)$, using a step size Δt :

$$\left. \begin{aligned}
 X_K &= AX_{K-1} + BW_K \\
 A &= \exp(-2\Delta t) \\
 B &= \sqrt{R_0(1-A^2)}
 \end{aligned} \right\} \text{where} \tag{22}$$

$$\left. \begin{aligned}
 E\{X_0\} &= 0 \\
 E\{X_0^2\} &= R_0.
 \end{aligned} \right\}$$

To complete the incoherent process generation, we need to transform X_K to a process with a bandpass spectrum. Let

$$Y_K = X_{1,K} \cos \omega t + X_{2,K} \sin \omega t, \tag{23}$$

where $X_{1,K}$ and $X_{2,K}$ are independent and as above (i.e., $N(0, \sqrt{R_0})$), stationary, with $R_{X_1}(\tau) = R_{X_2}(\tau) = R_X(\tau)$ and $t = K\Delta t$. The Y_K process is also Gaussian because it is a memoryless linear transformation of Gaussian processes. Further, it is stationary with the desired autocorrelation because:

$$\begin{aligned}
 E\{y_K\} &= \cos \omega t E\{X_{1,K}\} + \sin \omega t E\{X_{2,K}\} \\
 &= 0,
 \end{aligned}$$

and

$$\begin{aligned}
 E\{Y_K Y_{K+l}\} &= E\{(X_{1,K} \cos \omega t + X_{2,K} \sin \omega t) \\
 &\quad (X_{1,K+l} \cos \omega(t+\tau) + X_{2,K+l} \sin \omega(t+\tau))\} \\
 &= R_X(\tau) \cos \omega t \cos \omega(t+\tau) \\
 &\quad + E\{X_{1,K} X_{2,K+l}\} \cos \omega t \sin \omega(t+\tau) \\
 &\quad + E\{X_{2,K} X_{1,K+l}\} \sin \omega t \cos \omega(t+\tau) \\
 &\quad + R_X(\tau) \sin \omega t \sin \omega(t+\tau) \\
 &= R_X(\tau) (\cos \omega t \cos \omega(t+\tau) + \sin \omega t \sin \omega(t+\tau)) \\
 &= R_X(\tau) \cos \omega \tau.
 \end{aligned} \tag{24}$$

We now have a generation procedure for the two incoherent processes. Using four X_K processes we generate

$$\left. \begin{aligned}
 I_{P,K} &= \rho_I [X_{1,K} \cos(\omega K \Delta t) + X_{2,K} \sin(\omega K \Delta t)] \\
 I_{Q,K} &= \rho_I [X_{3,K} \cos(\omega K \Delta t) + X_{4,K} \sin(\omega K \Delta t)]
 \end{aligned} \right\} \tag{25}$$

where we have set $R_0 = 1$.

Antenna Pattern Effects

Our ECM applications simulations allow the use of various antenna patterns depending on the particular radar being simulated. Because of this, the multipath-effects simulation does not include antenna pattern effects explicitly. (The antenna pattern and multipath simulations are separate modules.) These effects must be introduced by the user once he has chosen an antenna pattern and determined a need to include multipath effects.

The effects of antenna patterns on the received signal are not well understood quantitatively and the author is not aware of any validated model for these effects. However, a simple model to account for these effects (which we have used in the simulation to date) is described in the following. We

assume that the two receive signals (\bar{D} and \bar{R}) are signals transmitted from two point sources located at the transmit radar and the sea surface specular point and that they are summed by the receive antenna with the associated antenna gains (Fig. 13). Because both \bar{D} and \bar{R} are representations of electric fields, to correctly account for antenna effects in such a model, amplitude gains must be used. This is done by producing a complex multipath factor F_{mp} normalized to the direct signal $\bar{D} = D \exp(j\theta_D)$. It is

$$F_{mp} = F \exp(j\theta) = F_R + jF_I. \quad (26)$$

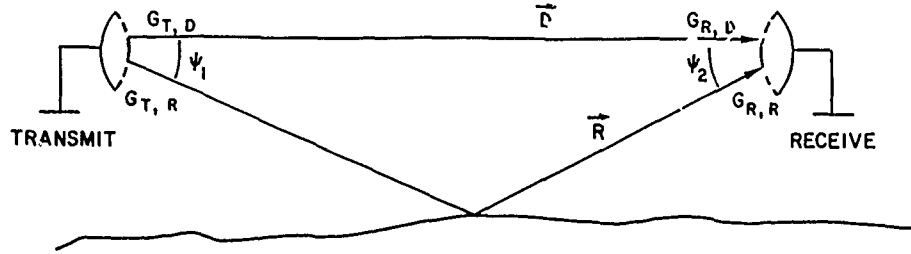


Fig. 13 -- Antenna gains schematic

Assuming unity antenna gains, the total received electric field becomes

$$\bar{T} = D[(1 + F_R) + jF_I] \exp(j\theta_D). \quad (27)$$

Now suppose the transmit and receive antennas have direct path amplitude gains $G_{T,D}$, and $G_{R,D}$, respectively, and reflected path amplitude gains of $G_{T,R}$ and $G_{R,R}$, respectively (all gains may be complex). Then the received electric field including antenna effects is represented by

$$\bar{T}_{ANT} = D[G_{R,D}G_{T,D} + G_{R,R}G_{T,R}F_{mp}] \exp(j\theta_D). \quad (28)$$

This simple model accounts for the qualitative fact that as the antennas illuminate less and less of the sea surface, the effect of multipath on the received signal should be reduced. However, it has been shown by Beard that this model is not quantitatively valid when the antennas do not fully illuminate the first Fresnel zone [3,15]. Even so, we have used this model of antenna patterns effects in the simulation for three reasons: at present there exists no validated model for these effects; this model does capture the qualitative effect of reducing the surface illumination; and it is a simple model to simulate. When an improved model is available, it will be incorporated in the simulation.

Moving Platform Multipath

The model as described to this point has assumed that the transmit and receive antennas were fixed relative to the earth.* However, since the situation where either one or both of the radars are moving is of prime interest to us in our studies, we now consider relaxing the fixed antenna constraint. The deterministic parts of the fixed model describe the deterministic moving platform multipath (MPM) effects by varying the geometry (antenna locations) with time. This in turn produces time variations in the associated deterministic parameters of the MPM model. However, the random components of the fixed model (the incoherent processes) are controlled by parameters that are determined by reflections from a fixed area of the sea surface. If either or both of the platforms move, then the area of reflection will no longer be fixed.

Because the author is unaware of any validated model for the incoherent component for MPM, we have developed a heuristic approach to modeling this component, which we will now discuss. First, it appears reasonable to assume that \bar{I}_P and \bar{I}_Q will remain independent, $N(0, \rho_i)$ processes and that ρ_i

*Relative motion has been anticipated in the previous sections; e.g. the ρ_i and ρ_c extrapolations.

will remain a function of only the sea roughness factor. The incoherent spectrum is directly determined by the sea surface structure. Because this structure is bandpass in nature (wavelengths occur within certain ranges for a given sea state) and because we assume that the surface is statistically stationary, we expect the MPM incoherent spectrum to remain bandpass in shape. The major area of sea surface contributing to the multipath signal is the area within the first several Fresnel zones [3,8]. Therefore, if the platforms are moving relative to one another, these zones are also changing location and/or size proportional to the rate of change of geometry of the platforms. If the zones are moving rapidly relative to the sea surface motion, then we can view the sea as fixed for a given period of time. If during this period the zones (sea surface area) change enough to cause a decorrelation of the received incoherent component, then one can associate the spectral bandwidths of the incoherent processes with a decorrelation distance (which translates to a decorrelation time) due to platform motions. Viewing the sea surface as fixed, with periodic structure centered about some dominant sea wavelength (a "typical" crest-to-crest length), we further suggest that the incoherent spectrum will have a dominant (center) frequency inversely proportional to the time required for the specular point to move from "dominant wave peak" to "dominant wave peak." Finally, we assume that the energy of the incoherent components will remain approximately constant for constant sea roughness factor.

Because our studies to date involving MPM (using, typically about Mach 1 closing velocities) have not required detailed knowledge of the incoherent spectrum, only the coherent induced nulling, we have implemented a simple approximation to this spectrum based on the above discussions. Our approximation is:

- (1) assume a bandpass spectral shape,
- (2) calculate a center frequency proportional to the ratio of specular point velocity and some "typical" sea wave length, and
- (3) calculate a bandwidth proportional to an estimate of the Fresnel zone decorrelation time.

Code 5750 is investigating the possibility of conducting an experiment involving a fixed radar and an airborne radar to collect data appropriate for further investigation of the MPM incoherent spectrum.

SUMMARY

In this report we have presented a simulation model of the effects of multipath in low grazing angle, over-water, radar scenarios. The purpose of the simulation is to generate a time series of data accurate to second-order statistics in its representation of experimentally measured effects, in particular, those effects measured by Code 5750 [10] which further confirm the fundamental vector representation made by Beard et al. [1]. The simulation model is based on the vector model of Beard et al., and utilizes various experimental results.

There are three major weaknesses in the model:

- (1) The inability to accurately account for antenna pattern effects when the first Fresnel zone is not uniformly illuminated.
- (2) The extrapolation of the scattering coefficient (coherent and incoherent) to regimes where they have not been experimentally verified.
- (3) The use of a model for the diffuse spectrum which has not been validated for moving platforms.

It should be noted that these weaknesses can all occur in moving platform scenarios.

This report describes an application of ongoing experimental and analytic research being conducted within Code 5750. Such research and changing application requirements will undoubtedly lead to modifications to the simulation, and so the simulation source code has been modularly designed to allow easy alterations of each component of the model. In particular, further analysis of Code 5750 multipath data could yield an improved model of the receive signal spectrum. As appropriate, any such modifications will be reported. Another report is being prepared that contains the FORTRAN source code listings used by Code 5750 to implement the simulation described in this report.

ACKNOWLEDGMENTS

The author gratefully acknowledges the fundamental contributions of Prof. J.S. Baras to this work. He introduced the author to stochastic modeling and multipath and it should be noted that authorship of both the concept of, and the approach to stochastic, multipath modeling belongs to him. Also, several conversations with Dr. C.I. Beard provided the author with valuable insight into the phenomena of multipath.

REFERENCES

1. C.I. Beard, I. Katz, and L.M. Spetner, "Phenomenological Vector Model of Microwave Reflection from the Ocean," IRE Trans., AP-4, pp. 162-167; April 1956.
2. C.I. Beard and I. Katz, "The Dependence of Microwave Radio Signal Spectra on Ocean Roughness and Wave Spectra," IRE Trans. on Ant. and Prop., AP-5, pp. 183-191; April 1957.
3. C.I. Beard, "Coherent and Incoherent Scattering of Microwaves from the Ocean," IRE Trans. on Ant. and Prop., AP-9, pp. 470-483, Sept. 1961.
4. J.S. Baras, "Multipath Effects Modeling," NRL Report in publication.
5. W.S. Ament, "Toward a Theory of Reflection by a Rough Surface," Proc. IRE, 41, pp. 142-146; Jan. 1953.
6. R.M. Brown and A.R. Miller, "Geometric-Optics Theory for Coherent Scattering of Microwaves from the Ocean Surface." NRL Report 7705, June 1974.
7. C.I. Beard, "Behavior of Non-Rayleigh Statistics of Microwave Forward Scatter from a Random Water Surface," IEEE Trans. on Ant. and Prop., AP-15, Sept. 1967.
8. F.E. Brooks, Jr., "Final Report of Radio Results for 1955 Gulf of Mexico Propagation Tests," Elec. Eng. Res. Lab., University of Texas Rep. No. 3-21, 31 March 1957.
9. D.E. Kerr (Editor), *Propagation of Short Radio Waves*, McGraw-Hill, New York, 1951.
10. A.D. Elia, R.D. Gurney, and D.Y. Northam, "Low Grazing Angle, Forward Scatter, Over-Water Multipath Measurements," NRL Report in publication.
11. W.J. McKune and H.W. Smith, "Comparison of Power Spectrum Estimates of Overwater Microwave Radio Signal and Associated Water Waves," Elec. Eng. Res. Lab., University of Texas Rep. No. 68; May 6, 1953.
12. G. Neumann, "On Wind Generated Ocean Waves with Special Reference to the Problem of Wave Forecasting," N.Y.U., Coll. of Eng., Res. Div., Dept. of Meteorol. and Oceanogr. Prepared for the Office of Naval Res., 1952.

NRL REPORT 8568

13. W.J. Pierson, Jr., G. Neumann, and R.W. James, *Practical Methods for Observing and Forecasting Ocean Waves*, Hydrographic Office Pub. No. 603, 1971.
14. A.E. Bryson and Y.C. Ho, *Applied Optimal Control*, Ginn and Co., Waltham MA, 1969.
15. C.I. Beard, "Remote Sensing of Ocean Significant Wave Height by Forward Scattering: Examples From L-Band Data," NRL Memorandum Report 3968, April 18, 1979.



DEPARTMENT OF THE NAVY
NAVAL RESEARCH LABORATORY
4555 OVERLOOK AVE SW
WASHINGTON DC 20375-5320

8 Aug 1997

IN REPLY REFER TO
5510
Ser 1221.1/0383

From: Commanding Officer, Naval Research Laboratory
To: Director, Foreign Disclosure and Technology Transfer
Division, Navy International Programs Office (IPO-11A4)

Subj: NRL REPORT 8568 (NAVY IPO CASE DOC-UK-6003-96)

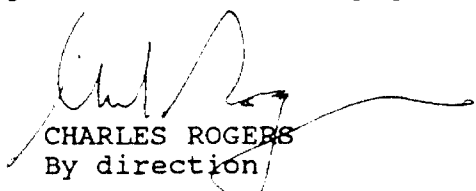
Ref: (a) Your ltr 5510 Ser 11A4/7U110501 of 26 Jun 97

Encl: (1) DERA (SSEW Dept) ltr of 11 Jun 97

1. Per reference (a), subject report was unclassified with "Distribution limited to U.S. Government Agencies only; test and evaluation; December 1981. Other requests for this document must be referred to the Commanding Officer, Naval Research Laboratory, Washington, D.C., 20375."

2. As requested by enclosure (1), a second review of the subject report was conducted and the distribution statement was changed to read: "Approved for public release; distribution is unlimited."

3. Please notify the requestor to make the appropriate changes to the cover page and the report documentation page of the subject report.


CHARLES ROGERS
By direction